Article

The International Journal of Robotics Research
0(0) 1–12

DOI: 10.1177/0278364913504247
ijr.sagepub.com

Anthropomorphic tendon-driven robotic hands can exceed human grasping capabilities following optimization

Joshua M Inouye[1] and Francisco J Valero-Cuevas[2]

Abstract

How functional versatility emerges in vertebrate limbs in spite of their anatomical complexity is a longstanding question. In particular, fingers are actuated by numerous muscles pulling on tendons following intricate paths. In contrast, the tendon-driven robotic hands with intuitive tendon routings preferred by roboticists for their ease of analysis and control do not perform at the level of their biological counterparts. Thus there is much debate on whether and how the anatomy of the human hand contributes to grasp capabilities. These parallel questions in biology and robotics arise partly because it is unclear how the number and routing of tendons offer functional benefits. We use a novel computational approach that analyzes tendon-driven systems and quantifies grasp quality to compare the precision grasp capabilities of thousands of robotic index finger and thumb designs vs. the capabilities measured in human hands. Our exhaustive search finds that neither the symmetrical designs sometimes preferred by roboticists nor randomly generated designs approach the grasp capabilities of the human hand (they are on average 73% weaker). However, optimizing for anatomically plausible asymmetry in joint centers, tendon routings, and maximal tendon tensions produces designs that can exceed the human hand by 13–45%, and outperform the preferred robotic designs by up to 435%. Thus, the grasp capabilities of prosthetic or anthropomorphic hands can be greatly improved by judiciously altering design parameters, at times in counter-intuitive ways. Moreover we conclude that, in addition to its other capabilities, the human hand's anatomy is very advantageous for precision grasp as it greatly outperforms numerous alternative robotic designs.

Keywords

Biologically-inspired robots, tendon-driven mechanism design, grasping, hand biomechanics

1. Introduction

The legendary complexity, intricacy, and functionality of vertebrate limbs in general, and the human hand in particular, are the perennial inspiration and envy of roboticists (Salisbury and Craig, 1982; Jacobsen et al., 1986; Jau, 1995; Ambrose et al., 2000; Massa et al., 2002). While all vertebrate limbs are actuated by muscles pulling on tendons (Valero-Cuevas, 2009), only relatively few robotic limbs have tendon-driven in favor of torque-driven hardware (Murray et al., 1994). It is interesting to note that anatomical limbs often have tendons that are routed with asymmetrical moment arms and unequal maximal tendon tensions. In contrast, roboticists prefer designs with relatively simple and symmetric routing and equal maximal tensions to simplify their design, analysis, and control. The overall performance and versatility of robotic hands severely lags behind that of their biological counterparts.

Due to the constraints of small size and light weight, robotic hands typically employ tendon-driven hardware. Some hand designs have been symmetrical (Jacobsen et al., 1986; Grebenstein et al., 2010), others have been asymmetrical (Salisbury and Craig, 1982; Carrozza et al., 2004), and still others have employed a bio-inspired approach that attempts to closely mimic the anatomy of the human hand (Folgheraiter and Gini, 2000; Vande Weghe et al., 2004; Shirafuji et al., 2012). However, none of them have employed systematic optimization procedures to enhance grasping capabilities.

There is much debate about how the anatomy of the human hand contributes to grasping capabilities and

[1]Brain-Body Dynamics Laboratory, Department of Biomedical Engineering, University of Southern California, USA
[2]Brain-Body Dynamics Laboratory, Department of Biomedical Engineering & Division of Biokinesiology and Physical Therapy, University of Southern California, USA

Corresponding author:
Francisco J Valero-Cuevas, Brain-Body Dynamics Laboratory, Department of Biomedical Engineering & Division of Biokinesiology and Physical Therapy, University of Southern California, Los Angeles, California 90089, USA.
Email: valero@usc.edu

whether it is 'optimized' in any sense. Similarly, there is much interest in understanding how to design robotic systems that can meet or exceed the performance of their biological counterparts. These parallel questions in biology and robotics arise in part because it is unclear whether and how the number and routing of tendons offer functional benefits.

Here we calculate the grasping capabilities of the human hand for index finger and thumb precision grasps, and compare them to the capabilities of thousands of different tendon-driven anthropomorphic designs. In particular, we explore the performance for precision grasp (sometimes also called pincer grasp, or tip-to-tip or precision pinch), which is a grasp modality essential for precision manipulation activities in humans (Cutkosky and Howe, 1990; Brand and Hollister, 1993; MacKenzie and Iberall, 1994) that is not achievable by most non-human primates (Schultz, 1968) unless they both can oppose the thumb and have the necessary phalangeal lengths. This is made possible by our novel computational approach that enables us to compute the grasp capabilities of tendon-driven systems of arbitrary complexity (Inouye et al., 2012a), and our ability to measure the fingertip forces produced by individual tendons in actual cadaveric hands. We find that i) anthropomorphic designs that optimize and incorporate apparently counter-intuitive anatomical features have superior capabilities to their unoptimized counterparts, and ii) the human hand is far superior to unoptimized robotic hand designs. These results compel and enable us to rethink our approach to the design of robotic systems, as well as inspire us to further investigate the functional consequences of the anatomy of the human hand.

2. Methods

2.1. Calculating human hand grasp quality

Given that there is no generally accepted computer model of the hand (Valero-Cuevas et al., 2009; Kutch and Valero-Cuevas, 2011, 2012), we opted for an experimental data approach to estimate the grasp capabilities of the human without making unnecessary modeling assumptions. To find the grasp quality of the human hand, we combined previously published cadaveric data (Valero-Cuevas et al., 2000; Pearlman et al., 2004) obtained from pulling on the tendons of actual cadaveric hands while measuring the vector output at the tips of the index finger and thumb. Having these vectors allowed us to use the same recently developed (Inouye et al., 2012a) computational method to calculate grasp quality as was used for the robotic fingers (see below). The cadaveric data are basis vectors of 3D fingertip forces in fingertip endpoint wrench space produced when tension is applied to each tendon individually proportional to their maximal tensions. These basis vectors are shown in Figure 1a. The feasible force set of each fingertip is built from these basis vectors and maximal tendon tensions using the approach outlined in Valero-Cuevas et al. (1998), Valero-Cuevas (2009), and Inouye et al. (2012a), and is shown in Figure 1b. The remaining procedure of intersecting the feasible force sets with friction cones (Figure 1c) and calculating the feasible grasp wrench set (Figure 1d) and associated global grasp metrics is described in Inouye et al. (2012a).

Since the grasp quality measures of characteristic length (i.e. the radius of a ball with the same volume as the grasp wrench set) and radius of the largest ball that can fit in the feasible wrench set (i.e. the distance from the origin of the feasible wrench set to its closest boundary, which is representative of the direction in which the grasp is weakest) are both linear measures and have identical units, we assign a single grasp quality metric to the human hand that simply sums the two measures. The radius of the largest ball is a measure of the largest magnitude of the forces and torques (collectively known as the wrench vector) that can be applied to the grasped object *in any 3D direction* to accelerate it, use it as a tool, or resist perturbations (Miller and Allen, 1999; Inouye et al., 2012a). Characteristic length is a measure of the average magnitude of the wrench that can be exerted or resisted by the grasp. Figure 1e shows how computation of the feasible object wrench predicts whether a grasp can be maintained against an external force.

The linear coefficient of friction is set to 0.5, and the ratio of the linear coefficient of friction to the rotational coefficient of friction is set to seven. Both of these values are in the range of physiologically reported friction coefficients for human fingertips (Kinoshita et al., 1997). The hand is assumed to grasp a ball of diameter 6 cm with the tip of the thumb on the bottom and the tip of the index finger on the top, as pictured in Figure 1c. This is the same methodology, grasp metric, hand posture, and friction coefficient as the ones used for the robotic hands.

2.2. Calculating anthropomorphic robotic hand grasp quality

We used the kinematic layout of the Shadow Hand (a tendon-driven, commercially available, anthropomorphic hand) to determine finger link lengths, fingertip placements, and postures for grasp. The kinematic layout and grasping posture of this anthropomorphic hand were selected because they closely resemble that of the human posture while still grasping the 6 cm ball, shown in Figure 2.

As is considered for the human hand (Valero-Cuevas et al., 2003; Valero-Cuevas, 2005; Santos and Valero-Cuevas, 2006), our robotic index finger has four degrees of freedom (three flexion–extension and one adduction–abduction), and the thumb has five (three flexion–extension and two adduction–abduction).

To allow a fair comparison of the grasp qualities of the anthropomorphic hand designs with those of the human hand, we adhered to the anatomical and kinematic constraints of the human hand. We set the coefficients of friction for the fingertips equal to those of human fingertips.

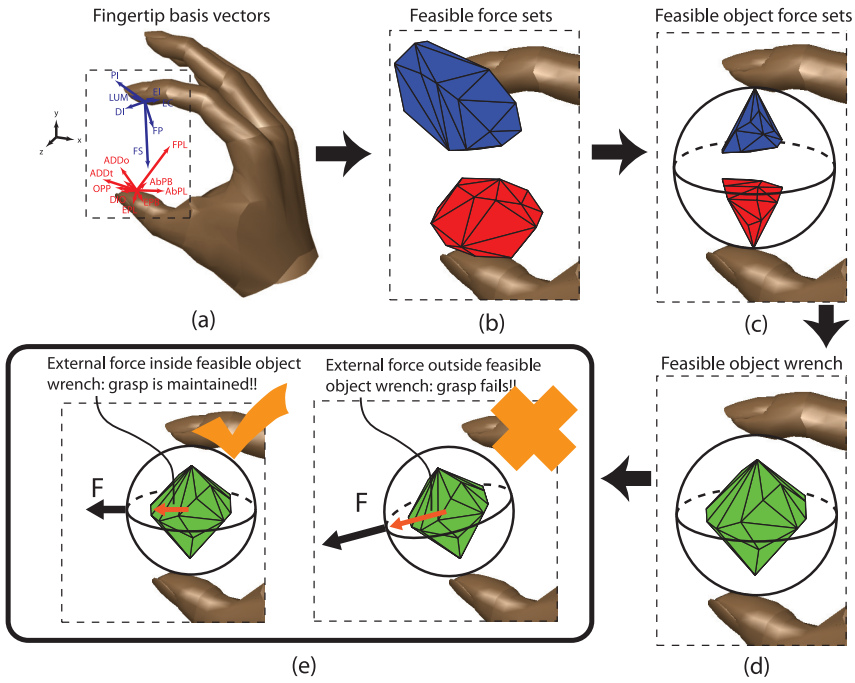

Fig. 1. Computation of human hand grasp quality. This is the same methodology and grasp metric that is used for the robotic hands. Index finger and thumb basis vectors and feasible force sets not equal scales. (a) Fingertip basis vectors. (b) Feasible force sets built from basis vectors. (c) Feasible object force sets: intersection of feasible force sets with friction cones. (d) Feasible object wrench (only 3D feasible forces shown). (e) Examples of maintained and failed grasps.

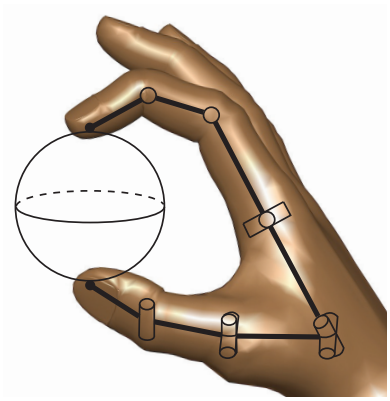

Fig. 2. Anthropomorphic hand grasp.

Moreover, the sum of the maximal tendon tensions for each finger was set to that of human fingers: 764 N for the index finger and 478 N for the thumb (Valero-Cuevas et al., 2000; Pearlman et al., 2004). The reason is that muscle strength is related to its cross-sectional area (Zajac, 1989). Thus, regardless of how many tendons each index finger or thumb has, the human forearm and hand have a given volume and therefore a fixed total maximal muscle force available to drive the hand. Also, the moment arm values were constrained so that the size of each joint would not exceed that of the corresponding human joints. The moment arms for the human index finger and thumb were taken from the literature (Valero-Cuevas et al., 1998, 2003), and the implied 'joint diameters' (i.e. the maximal differences between moment arm values for a joint) were used to constrain the joint diameters for the anthropomorphic hand designs. For example, the maximal positive moment arm value for the index finger metacarpophalangeal (MCP) joint is 13.2 mm and the maximal negative moment arm value for the index finger MCP joint is −7.8 mm (Valero-Cuevas et al., 1998). Therefore, the 'joint diameter' is 21.0 mm. The anthropomorphic hand designs were constrained so that their joint diameters were equal to those of their human hand counterparts. The joint diameters are shown in Table 1.

Moreover, after some preliminary testing and optimization, we found that using only the above constraints resulted in optimized designs that were extremely good at grasping (more than 100% greater grasp quality than the human hand), but were extremely poor at exerting force in all directions. The ability of a fingertip to produce force in all directions can be measured by the maximum isotropic value, or MIV (the maximal force that can be exerted in all directions, described in Finotello et al., 1998). Intuitively, it is the radius of the largest ball, centered at the origin of the feasible force set, that can fit inside the feasible force set.[1] For some directions, namely extension, the fingers in optimized designs could only produce less than 0.05 N. This was due to the optimization process placing all the emphasis on flexion force and none on extension force. Since this

Table 1. Maximal joint diameters (i.e. differences between largest moment arms for each joint) according to data obtained from the literature.

	Joint	Joint diameter (mm)
Index finger	MCP adduction–abduction	10.9
	MCP flexion–extension	21.0
	PIP flexion–extension	9.25
	DIP flexion–extension	5.14
Thumb	CMC adduction–abduction	35.6
	CMC flexion–extension	40.4
	MP adduction–abduction	15.5
	MP flexion–extension	20.2
	IP flexion–extension	11.0

MCP: metacarpophalangeal; PIP: proximal interphalangeal; DIP: distal interphalangeal; CMC: carpometacarpal; MP: metacarpophalangeal; IP: interphalangeal.

is such a low force, and so unreasonable compared to the human hand, we felt it was necessary to constrain the MIV for anthropomorphic finger designs to be at least that of the human fingers. The MIV of the human index finger is 2.89 N, and 5.37 N for the thumb (Valero-Cuevas et al., 2000; Pearlman et al., 2004). This ensures the ability to release a grasp and for each finger to exert at least as much force in all directions as human fingers.

2.3. Optimizing anthropomorphic robotic hand grasp quality

We used three separate steps for initializing and optimizing anthropomorphic robotic hand designs:

1. An initial random search of the parameter space using a Monte Carlo search on the parameters of the structure matrices that define tendon routings and crossover operations of best designs.
2. Optimization step 1: Markov-chain Monte Carlo search to adjust the joint centers of rotation.
3. Optimization step 2: Markov-chain Monte Carlo search on the distribution of maximal tension among tendons.

Monte Carlo over the structure matrices was used due to the fact that the feasible force sets of the fingers, and therefore the grasp quality of the hand, are complex functions of the high-dimensional structure matrices. The Markov-chain Monte Carlo methods were deemed appropriate due to the high dimensionality of the system and the large computational cost of computing approximate gradients (e.g. using steepest-ascent, Newton's method, etc.).

2.3.1. Original Monte Carlo search on structure matrices To find tendon layouts on which to perform optimization, we first performed a Monte Carlo exploration of the space of structure matrices for the fingers; see Figure 3. We explored the space of four different tendon designs: $N+1$, $N+2$, $N+3$, and $2N$, where N is the number

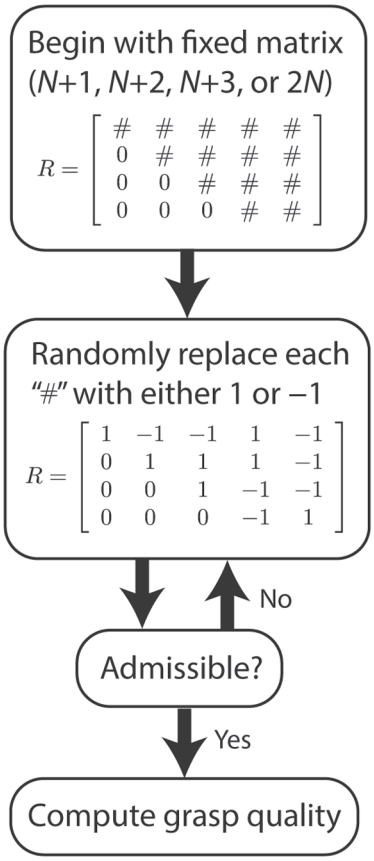

Fig. 3. Procedure for finding randomized designs via Monte Carlo sampling.

of degrees of freedom for each finger. For tendon-driven systems, $N+1$ is the minimal number of tendons needed to have a controllable finger (Valero-Cuevas, 2009). To do so, we randomly generated 1000 pairs of admissible structure matrices (one for the index finger, one for the thumb) for each of the four designs. These structure matrices were in a pseudotriangular form, as described in Lee and Tsai (1991). The process of generating a random matrix for each finger is illustrated in Figure 3. We first began with a fixed matrix consisting of some zeros and some '#' entries where non-zero moment arm values would be inserted. Next, we randomly replaced each '#' with either 1 or -1. We then checked conditions for the controllability of a tendon-driven finger (also described in Lee and Tsai, 1991). Basically, we checked if the matrix was full rank, made sure there was at least one sign change in each row (i.e. that each joint had an extensor and flexor tendon), and tested if a null-space basis vector found via singular value decomposition existed whose elements all had the same sign (to make sure the finger could hold a posture).[2] If the structure matrix was found to satisfy these conditions, we would calculate the MIV of the feasible force set associated with that structure matrix of each finger. If the structure matrix did not meet all these admissibility criteria, we randomized the structure matrix again. After a pair of admissible structure matrices were found for the

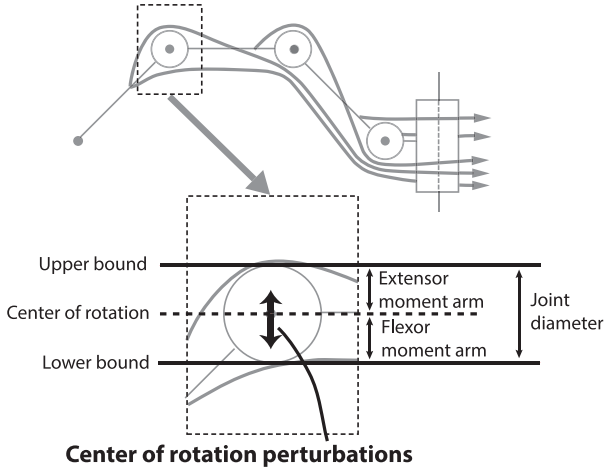

Fig. 4. Illustration of perturbations of the joint center of rotation.

index finger and thumb, we calculated the grasp quality for the 'hand design' that used that pair. We found 4000 randomized hand designs and calculated the grasp quality of each.

2.3.2. Optimization step 1: Optimization of joint centers of rotation As optimization of all 4000 Monte-Carlo-generated hand designs was not practical, we had to choose a small number on which to perform optimization procedures. We did this based on the fingers with the highest MIV. We took the 10 index finger structure matrices and the 10 thumb structure matrices with the highest MIVs (regardless of the number of tendons) and crossed them over with each other, creating 100 additional combinations of index finger and thumb structure matrices (i.e. hand designs). This crossover operation is a standard method in genetic algorithms. The grasp quality was then calculated for these additional 100 hand designs produced from crossover operations and the 10 hand designs with the highest grasp qualities were chosen for optimization. We reasoned that the structure matrices with the highest MIVs would be the most flexible during the later stages of the optimization. In addition, this guarded us from designs with the very highest grasp quality that either did not meet the minimum MIV requirements, or were very close to violating them.

The first optimization procedure performed on the 10 chosen designs involved the joint centers of rotation. This is in the sense of moment arms on one side of the joint becoming larger than those on the other side of the joint, with the total range of the moment arms being equal to the joint diameter.[3] A greedy Markov-chain Monte Carlo algorithm was employed on each finger separately. The initial centers of rotation were in the middle of the joints and the grasp quality was calculated. The index finger joint centers of rotation were then perturbed simultaneously (all four at once) by independent, normally distributed random numbers u_i (for the ith joint) with zero mean and a standard

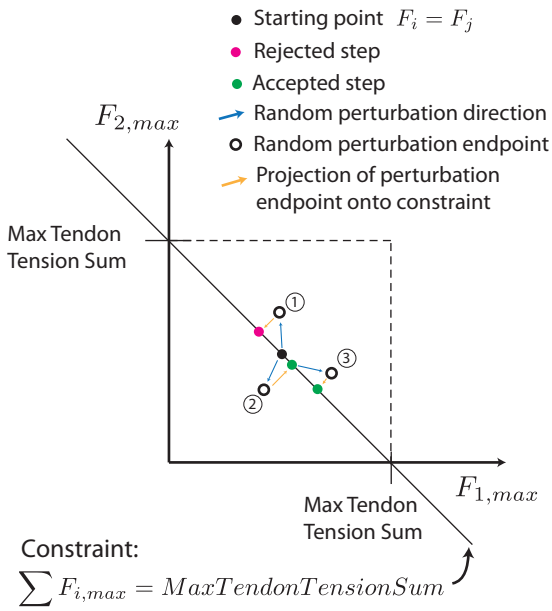

Fig. 5. Illustration of the Markov-chain Monte Carlo algorithm for distribution of maximal tendon tensions.

deviation of 2% of the joint diameter. The centers of rotation were constrained so that they did not go outside the joint diameters, and a reflection technique similar to that in Santos et al. (2009) was used. Perturbation of the center of rotation is demonstrated in Figure 4.

2.3.3. Optimization step 2: Optimization of maximal tendon tensions The last step in our optimization process involved performing a similar Markov-chain Monte Carlo exploration of the maximal tendon tension distribution across tendons. Starting with all the tendons having equal maximal tendon tensions, we perturbed the distribution of the maximal tendon tensions using a multivariate normal distribution with a standard deviation of 2% of the maximal tendon tension sum (764 N for the index finger and 478 N for the thumb; values obtained from Valero-Cuevas et al. (2000) and Pearlman et al. (2004)). This perturbation was effectively like one inside an n-dimensional hypercube in the positive orthant with side length equal to the maximal tendon tension sum, where n is the number of tendons for each finger. After perturbation inside the hypercube, we projected the point onto the hyperplane given by the following equation:

$$\sum_{i=1}^{n} F_{i,max} = MaxTendonTensionSum \qquad (1)$$

where $F_{i,max}$ is the maximal tension of tendon i. This gave us a new distribution of maximal tendon tensions, and we then evaluated the grasp quality. If it was higher, we took that point as the starting point for the next perturbation. The same reflection technique as that in the previous section was used. The overall process is shown graphically for a simplified two-tendon example in Figure 5.

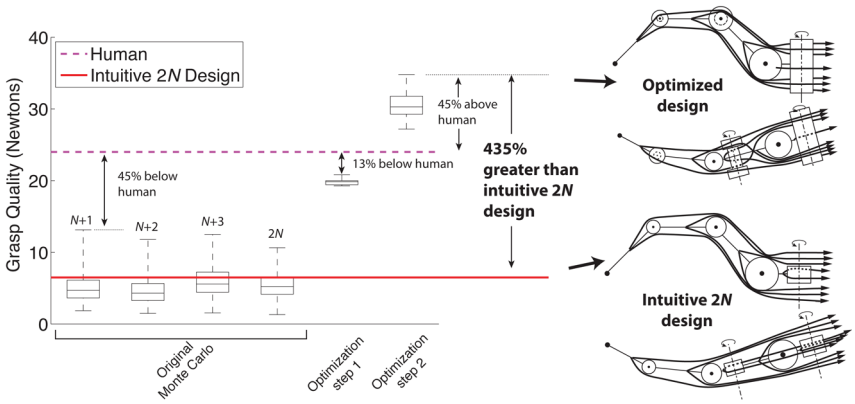

Fig. 6. Comparison of human grasp quality with box plots of anthropomorphic hand designs. N is the number of degrees of freedom of each finger. The original Monte Carlo searches the set of all possible flexor/extensor routings for the index finger and thumb. Optimization step 1 is for the joint centers of rotation. Optimization step 2 is for the distribution of maximal tendon tensions. Distribution of maximal tendon tensions is not shown, for clarity. Moment arms for each joint shown very roughly to scale.

A detailed explanation of the effects of different structure matrices and distributions of maximal tendon tensions on the kinetostatic (i.e. force-production) capabilities of manipulators and biological hands can be found in Lee and Tsai (1991), Ou and Tsai (1993, 1996), Tsai (1995), Finotello et al. (1998), Valero-Cuevas (2009), and Inouye et al. (2012a).

3. Results

Figure 6 summarizes the results for grasp quality. These results include both the randomized and the optimized designs with different numbers of tendons, both before and after Markov-chain Monte Carlo optimization procedures. It should be noted that the original Monte Carlo box plots are not in series, but the optimization steps are in series after allowing selection from all four categories of structure matrices, as described in Section 2.

We see that an intuitive robotic design with $2N$ tendons (which control either only flexion–extension or only adduction–abduction) with symmetric moment arms and equal maximal tensions found does very poorly in relation to the human hand. However, adding the anatomically tenable features of asymmetric moment arms (by shifting the centers of rotation of the joints) and unequal maximal tendon tensions (but keeping within anatomical finger girth and the total sum of muscle strengths) produces designs whose grasp quality exceeds that of the human hand. In addition, we see that intelligently choosing parameters for hand design can result in grasp quality that is 435% higher than this intuitive $2N$ design!

3.1. Randomly selected designs

We see from Figure 6 that there is a large range of grasp qualities for these fully controllable hands. The figure shows the performance of designs with different numbers of tendons ($N + 1$, $N + 2$, $N + 3$, and $2N$, where N is the number of each finger's kinematic degrees of freedom: four for the index finger and five for the thumb). Note that in these cases the same total maximal muscle strength was distributed among all tendons as a means to allow for the fact that the human forearm and hand have a given volume, and therefore total muscle force available to drive the hand. Figure 7 shows two tendon routings for the index finger. Figure 7a shows the best index finger crossover design that was selected for optimization. We do not show the design that had the highest grasp quality of the randomly selected designs because it did not perform as well as others after optimization. Figure 7b shows an index finger tendon routing that produced a very poor grasp quality before optimization. For the purposes of kinematic clarity, the finger adduction–abduction (i.e. side-to-side) axis was considered to be immediately proximal to the perpendicular axis of the first flexor–extensor joint, as demonstrated in Figure 7a.

3.2. Optimization of joint centers of rotation and distribution of maximal tendon tensions

We further optimized the top 10 hand designs produced from the crossover operations. We used 150 iterations for the joint centers of rotation optimization for each finger separately. Results from using 10 random starting locations for the index finger within the space of allowable centers of rotation as well as a starting location in the middle of all the joints showed that the random seeds all converged to roughly the same point, with a small range in final grasp quality, as shown in Figure 8a. The range of grasp qualities for the random seeds was 16.08–16.19 N, or 0.7% of the mean.

As is customary when multiple Markov chains converge to a same general location, we deemed the 150 iterations to allow sufficient convergence for our study (Santos and Valero-Cuevas, 2006). Thus, running multiple Markov chains for each design was unnecessary. It should be noted that although all 10 random seeds were randomly selected from a uniform distribution in the theoretically allowable

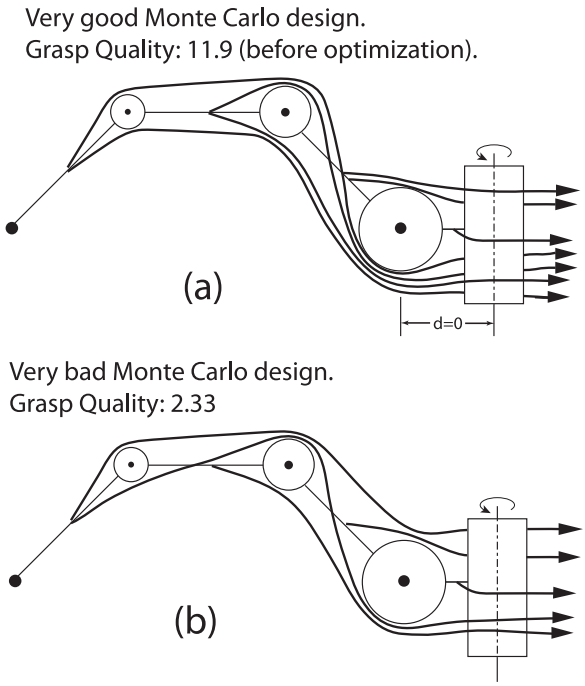

Fig. 7. Two sample index finger tendon routings. Moment arms not drawn to scale and only show which sides of the joints the tendons cross. (a) Best crossover index finger tendon routing after optimization. (b) Unoptimized tendon routing that produced a very low grasp quality.

range (i.e. within the unit hypercube; two selected dimensions shown in Figure 8a), some seeds did not meet the minimum MIV requirements, and they were discarded and re-selected. The final solutions shown in Figure 8a are slightly dispersed in the proximal interphalangeal (PIP) joint center of rotation, but the range of grasp qualities is very small, suggesting a very flat fitness landscape in that vicinity along that direction.

In addition, we see the progress of the best found result versus the iteration number in Figure 8b. Graphically, it can be seen that over the course of 150 iterations, most of the improvement (almost 85%) comes in the first 50 iterations. While we allowed the optimization to run for three times that long, we felt that any more iterations would result in diminishing returns and marginal improvements in results. It took about 3.7 s, on average, to compute the grasp quality for each iteration. This first optimization of joint centers of rotation produced designs with grasp qualities between 19.3 N and 20.8 N, falling short of the human grasp quality by 13–20%, and 17% on average, as shown in Figure 6.

We implemented that same procedure to optimize for the distribution of maximal tendon tensions for each finger separately (i.e. 150 iterations). The result of using 10 random seeds produced grasp qualities with a very small range (5.5% of the mean). Again, this indicated that multiple chains were unnecessary for our purposes. The plot of typical optimized grasp quality versus iteration number was very similar to that shown in Figure 8b (in fact, with 96% of the improvement coming within the first 50 iterations), and therefore the 150 iterations were deemed sufficient. This second optimization of maximal tendon tension distributions produced designs with grasp qualities that were on average 55% higher than those with evenly distributed maximal tendon tensions.

Moreover, this second optimization of the 10 best crossover designs produced hands whose grasp quality exceeded that of the human hand by 13–45%, as shown in Figure 6. The tendon routing for the index finger and thumb, the distribution of maximal tendon tensions, and the feasible force sets for the best two designs and the human hand design are shown in Figure 9. Interestingly, the feasible force set of the human index finger is much larger than that of the thumb, while the opposite is true of the optimized designs. It can be seen that the optimization caused the feasible force sets to be weighted more heavily toward flexing in the palmar direction (i.e. the direction of force production during grasping).

4. Discussion

In this study, we have successfully compared thousands of random and optimized hand designs to the human hand in terms of quality of precision grasp. We demonstrate the use and power of the methodology developed in Inouye et al. (2012a) to compare and optimize hand designs in a high-dimensional parameter space, while still adhering to specific anatomical and design constraints. Our study concentrated on the grasp of one object of a reasonable size in a specific posture. We did not perform extensive sensitivity analysis on certain factors such as differing postures, finger placements, friction coefficients, surface curvatures, object shapes, etc. The methodology that we employed would allow simulations to take most of these factors into account, but we felt that this was not necessary to arrive at the conclusions that i) anthropomorphic designs that incorporate apparently counter-intiuitive anatomical features have superior capabilities to their unoptimized counterparts, and ii) the human hand is far superior to unoptimized robotic hand designs. In addition, we do not include the force–length interaction of musculotendons, known to affect muscle force production as a function of posture (Zajac, 1989).

To the best of our knowledge, we are the first to be able to clearly compare the upper limit of the mechanical capabilities for precision grasp between thousands of anatomically feasible tendon-driven robotic designs and the human hand.[4] While one can argue that few tasks require using maximal force capabilities because many activities of daily living only require low forces, having a mechanical structure that can produce large forces is desirable for multiple reasons. For example, if the finger mechanism has a high gain (i.e. large grasp forces per unit input of muscle force) then those everyday tasks will require lower muscle forces

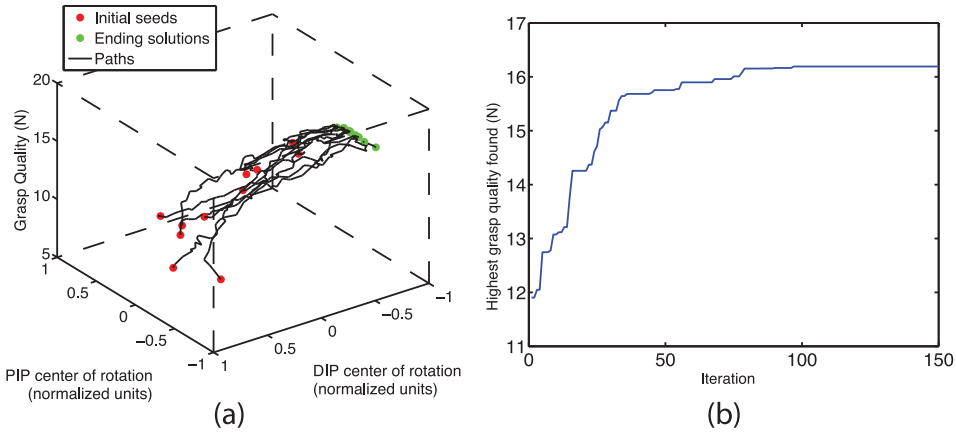

Fig. 8. Markov-chain Monte Carlo optimization of asymmetry in joint centers of rotation. (a) Visualization of optimization paths of 10 random seeds and one center seed. (b) Optimization progress over 150 iterations.

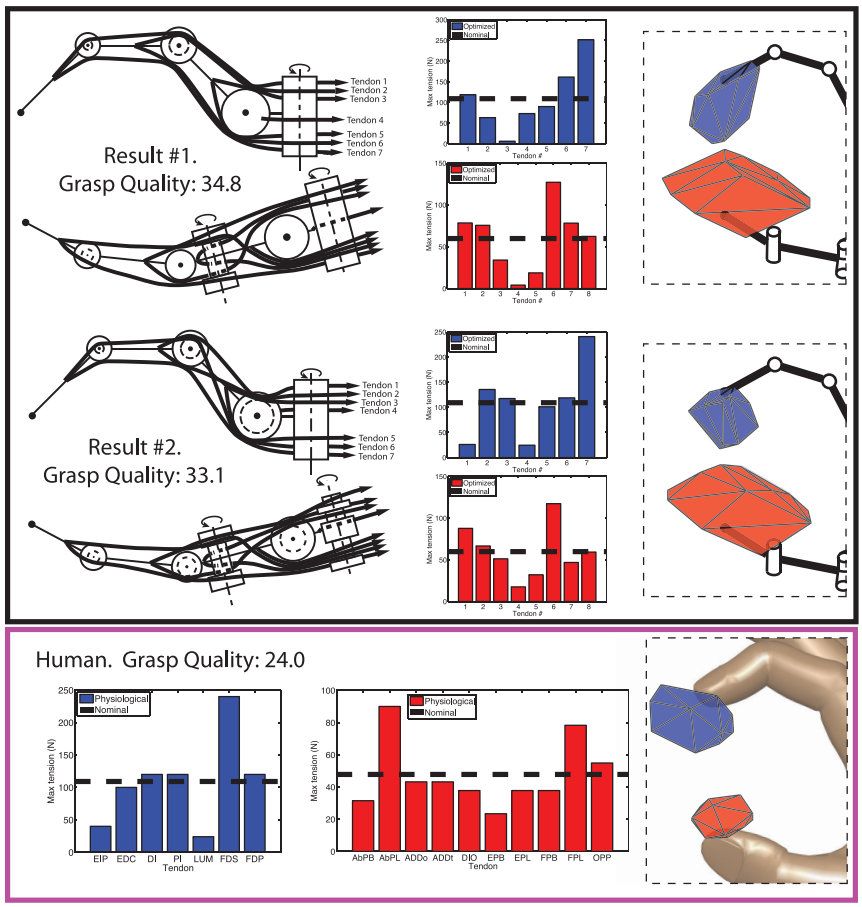

Fig. 9. Index finger tendon layout, maximal tendon tension distribution, and feasible force sets for top two optimized designs and the human hand. Tendon layouts shown roughly to scale. Feasible force sets shown to scale.

and metabolic costs, and induce smaller stresses on the tissue and joints. In addition, such mechanical structures will have a greater safety margin and require smaller force actuators (be they motors or muscles), as well as being more functional when the person is either developing as a child, or weakening with disease or aging.

The results obtained in this study are made possible by the combination of recent innovations that made this historically complex problem tractable. First, our study is unique in that we have only recently been able to calculate task-independent grasp quality metrics for tendon-driven systems of arbitrary complexity (Inouye et al., 2012a).

Second, the fact that our data for precision grasp for the human hand come from cadaveric experiments provides substantial advantages to our study, its results, and its conclusions. Recall that the feasible grasp set for the human hand was created from data measured by pulling on actual anatomical hands in those same postures we studied in the robotic designs (see Section 2), and is therefore strictly empirical. Thus there was no need make assumptions about tendon-force transmission or create a computer model of the human hand. A trustworthy computer model of the hand remains an elusive goal (Valero-Cuevas et al., 2009; Kutch and Valero-Cuevas, 2011, 2012), which is exacerbated by the complex tendon-tension transmission through the extensor mechanisms of the index finger (Valero-Cuevas et al., 2007; Kurse et al., 2012). Thus, by directly measuring the vector output at the tips of the index finger and thumb when pulling on individual tendons, we have as good an estimate of the grasp capabilities of the hand as is currently possible. These two innovations allowed us to directly compare grasp capabilities of actual anatomical specimens with thousands of alternative robotic designs, with the same units and quality metrics.

We note that in any useful biological or robotic hand, the mechanics *and* control must both be considered and developed. The best control algorithms cannot perform any task that the mechanics do not allow. Conversely, a globally optimal hand from a mechanics standpoint is useless without effective control to implement these capabilities. The consequences to the control of various designs have not been considered in this paper, and this is the subject of related and future work: is a tendon-driven hand with an optimized grasp quality difficult to control? Or is it that engineers find them difficult to control given the limitations of the contemporary interpretation and phrasing of the control problem? Recent work (Theodorou, 2011) suggests that a combination of stochastic optimal control with reinforcement learning makes tractable the difficult problem of controlling tendon-driven systems (for a description of the difficulties of classical optimal control with tendon-driven systems see Valero-Cuevas et al., 2009). Other work considers optimization of tendon tensions for adequate controllability and operation of a robotic system under various constraints (some of which are not considered in this study) (Bicchi and Prattichizzo, 2000; Gabiccini et al., 2011). Further research on the integration of optimized mechanics and optimized control will increase the performance of tendon-driven systems.

One exciting conclusion of this study is that utilizing even fairly simple Monte Carlo exploration and optimization techniques can compare robotic and anatomical hands, and provide clear means to improving the grasp quality of robotic hands by nearly one order of magnitude (435% increase) when compared with the intuitive $2N$ design (shown in Figure 6) that simplifies analysis and control (e.g. two tendons per joint, symmetric moment arms, and equal maximal tendon tensions). Thus, this study has directly applicable implications for the design of prosthetic and industrial robotic hands for precision grasp, that include the use of perhaps counter-intuitive (yet mechanically explainable in hindsight) asymmetric and apparently complex tendon routings. Clearly, the repertoire of tasks a hand fulfills goes far beyond precision grasp, or even grasp and manipulation in general. Thus, in the general design case where the hand will perform a variety of tasks in unstructured environments, multiple grasp metrics (like those here, and in Balasubramanian et al., 2010; Inouye et al., 2012a) must be used to compare the fitness of various designs. However, it is also clear that precision manipulation with the fingertips is an important category that should be considered if the hand is to be at all dexterous (Salisbury and Craig, 1982; Jacobsen et al., 1986; Jau, 1995; Ambrose et al., 2000; Massa et al., 2002); thus our chosen task has face validity and serves as a good first comparison and evaluation of multiple tendon routings that will naturally enable future work in other grasp domains.

By the same argument, it is noteworthy that our analysis clearly shows that the human hand is, at the very least, very anatomically advantageous for precision grasp. Given the large repertoire of competing functional requirements that makes the hand such a central part of our identity as a species (Porter et al., 1993; MacKenzie and Iberall, 1994; Wilson, 1999), we somewhat expected to find the human hand to have only moderate precision grasp capability compared to alternative robotic designs. Therefore it is surprising and interesting to see that the human hand greatly outperforms thousands of alternative robotic designs (both random and optimized). In addition, this kind of precision grasp is only achievable in those few primates (Schultz, 1968) that have the necessary phalangeal lengths and joint configurations to completely oppose the thumb and create the closed kinematic chain. This in turn suggests that being able to grasp with the fingertips is in fact an important functional category in humans to enable precision manipulation for successful everyday life.

In spite of its limitations that do not challenge our main results or conclusions, our work is only the first example of optimization techniques that can now be employed to explore the full grasp capabilities of tendon-driven systems. Varying the optimization techniques, parameters, or orders of steps would affect the upper limit of the grasp qualities found. One example is to only optimize maximal tendon tensions and retain constant moment arms if one wants to consider robotic hand designs with circular pulleys of a single diameter for each joint. As another example, we could have used a complete Monte Carlo search on all the parameters at once or in groups (structure matrix, maximal tendon tensions, and moment arms). However, given the extremely high dimensionality of the problem, many of the initial 4000 designs would have poor distributions of moment arms and maximal tensions. Given the vast number of ways that the search and optimization procedures could have been carried out, we were restricted to a procedure that we felt would

give good results in a reasonable amount of computational time. As described in Section 2, this was to initially select the best structure matrices for optimization. It is possible that other designs not selected for optimization could have exceeded our best design after optimization. However, note that our main conclusions do not hinge on finding a global optimum; we felt that our results would not be significantly affected by spending much more time and effort trying to obtain, say, a 10–20% higher grasp quality than we found for the optimized designs. Future work can focus on optimizing robotic designs with structure matrices that are not necessarily upper-triangular, as in Sheu et al. (2009).

A difference between our robotic designs and the human hand can be seen in Figure 9, where the optimized thumb feasible force sets were much larger than that of the human. One explanation for this is that all the tendons in the optimized designs were at the boundaries of their joint diameters. In the human, the extreme moment arms defined the joint diameters, but the rest of the tendons typically were not nearly as large as these extremes. For example, the maximal human MCP flexion moment arm was 13.2 mm and the maximal extension moment arm was 7.77 mm, giving a joint diameter of 21.0 mm. If this were an optimized robotic hand, all the flexion moment arms would be 13.2 mm and all the extension moment arms would be 7.77 mm. However, in the human, given anatomical constraints, only one flexor has a moment arm this large and only one other extensor has a moment arm this large. The other four tendons have smaller moment arms at this axis. Due to the fact that the joint diameters for the thumb carpometacarpal (CMC) joint were quite large, the optimized designs were able to take full advantage of having many large moment arms, while the human thumb only used two moment arms to the maximum extent possible.

As demonstrated by the results, the optimizations for grasp produced finger designs with feasible force sets heavily weighted toward the object (i.e. optimized for flexion). The human fingers also have feasible force sets that tend to be optimized for flexion. A few of our other studies have considered optimization of the force-production capabilities of tendon-driven robotic fingers and manipulators, but the fitness metric used in those studies was maximal isotropic force (Inouye and Valero-Cuevas, 2012; Inouye et al., 2012b). Grasp quality metrics with feasible force sets optimized for maximal isotropic force could be decent, but they would certainly increase if they were optimized for flexion force that creates a large asymmetry in the feasible force set (as evidenced by the optimized designs in this study).

The potential limitations of the fidelity of a cadaveric hand in reflecting the mechanics of the live hand have been raised and addressed in our prior work (Valero-Cuevas et al., 2000; Pearlman et al., 2004). In spite of the potential nonlinearities and inaccuracies in such measurements (both inherent to the hand and as a result of experimental error), we find that the human hand greatly outperforms unoptimized robotic designs that are subject to human limitations. Future experimental paradigms or modeling environments that mitigate or circumvent the limitations of cadaveric testing can likely only strengthen our conclusions that the hand has outstanding grasp capabilities when compared with unoptimized anatomies and topologies.

Lastly, although we constrained the robotic hand specifications, such as anthropomorphic dimensions and constant sum of maximal tendon tensions, to allow for a fair comparison to the human hand, robotic hands are generally not constrained to all of these human specifications. However, the principles of minimizing hand size (e.g. joint diameters) and actuator size and weight (e.g. maximal tendon tensions) are beneficial for many tendon-driven robotic applications such as minimally invasive surgery, prosthetic hands, and robotic manipulators. Therefore, optimizations for different robotic systems should harness their advantages over human anatomy to the fullest extent possible in the design process, while still conforming to constraints that guarantee correct and controllable operation (Bicchi and Prattichizzo, 2000; Gabiccini et al., 2011).

Our results show that the human hand and robotic hand designs employing human-like features (such as optimized asymmetry) vastly exceed the performance of their unoptimized counterparts. The outstanding performance of the human hand inspires us to rethink our approach to the design of robotic hands in particular and robotic systems in general.

Acknowledgements

The authors gratefully acknowledge the useful discussions with J Kutch.

Funding

This material is based upon work supported by the NSF (grant number EFRI-COPN 0836042), the NIDRR (grant number 84-133E2008-8), and the NIH (grant numbers AR050520 and AR052345): grants made to FJ Valero-Cuevas.

Notes

1. Note that this ‘largest ball’ is for the feasible force set and measures the MIV, which is different from the largest ball grasp quality metric, which is calculated from the grasp wrench set.
2. These conditions correspond to fully actuated robotic fingers. We did not consider underactuated robotic fingers in our study as they are not capable of approaching the dexterity of human fingers. However, we do point out that the development of underactuated fingers is a large research area that has drawn considerable interest due to the simplicity of their control.
3. While a simplified explanation of our joint constraint is that the center of rotation was perturbed, this would actually imply a non-linear relation between moment arms and joint angles. However, in our analysis we actually assume constant (but not necessarily equal) moment arms for each side of the joint. A non-linear relation would not affect our results since we only tested the grasp in one position, but it could certainly affect

grasp quality more if the grasp configuration was changed dramatically.

4. One study has calculated a task-specific grasp quality metric for a specific robotic hand and compared it with the human hand (Fu and Pollard, 2006), but the grasp limit has not been found since they do not calculate the full grasp wrench set. Another study has compared human fingers with optimized robotic fingers, but they do not calculate grasp quality (Pollard and Gilbert, 2002).

References

Ambrose RO, Aldridge H, Askew RS, et al. (2000) Robonaut: NASA's space humanoid. *IEEE Intelligent Systems and Their Applications* 15(4): 57–63.

Balasubramanian R, Xu L, Brook PD, et al. (2010) Human-guided grasp measures improve grasp robustness on physical robot. In: *2010 IEEE International conference on robotics and automation (ICRA)*, pp. 2294–2301.

Bicchi A and Prattichizzo D (2000) Analysis and optimization of tendinous actuation for biomorphically designed robotic systems. *Robotica* 18(1): 23–31.

Brand PW and Hollister A (1993) *Clinical Mechanics of the Hand*. St. Louis, USA: Mosby Year Book.

Carrozza MC, Suppo C, Sebastiani F, et al. (2004) The spring hand: Development of a self-adaptive prosthesis for restoring natural grasping. *Autonomous Robots* 16(2): 125–141.

Cutkosky MR and Howe RD (1990) Human grasp choice and robotic grasp analysis. *Dextrous Robot Hands*. New York: Springer, pp. 5–31.

Finotello R, Grasso T, Rossi G, et al. (1998) Computation of kinetostatic performances of robot manipulators with polytopes. In: *Proceedings of the 1998 IEEE International conference on robotics and automation*, pp. 3241–3246.

Folgheraiter M and Gini G (2000) Blackfingers an artificial hand that copies human hand in structure, size, and function. *Proceedings of IEEE Humanoids*. In: First IEEE-RAS International conference on humanoid robots.

Fu JL and Pollard NS (2006) On the importance of asymmetries in grasp quality metrics for tendon driven hands. In: *2006 IEEE/RSJ International conference on intelligent robots and systems*, pp. 1068–1075.

Gabiccini M, Branchetti M and Bicchi A (2011) Dynamic optimization of tendon tensions in biomorphically designed hands with rolling constraints. In: *Proceedings of the 2011 IEEE International conference on robotics and automation*, pp. 2698–2704.

Grebenstein M, Chalon M, Hirzinger G, et al. (2010) Antagonistically driven finger design for the anthropomorphic DLR hand arm system. In: *2010 IEEE-RAS International conference on humanoid robots (Humanoids)*, pp. 609–616.

Inouye J and Valero-Cuevas FJ (2012) Asymmetric routings with fewer tendons can offer both flexible endpoint stiffness control and high force-production capabilities in robotic fingers. In: *2012 IEEE RAS & EMBS International conference on biomedical robotics and biomechatronics (BioRob)*, pp. 1273–1280.

Inouye J, Kutch J and Valero-Cuevas F (2012a) A novel synthesis of computational approaches enables optimization of grasp quality of tendon-driven hands. *IEEE Transactions on Robotics* 28(4): 958–966.

Inouye JM, Kutch JJ and Valero-Cuevas FJ (2012b) Optimizing the topology of tendon-driven fingers: Rationale, predictions and implementation. In: Cutkosky M, Dollar A and Howe R (eds) *The Human Hand: A Source of Inspiration for Robotic Hands* (*Springer Tracts in Advanced Robotics*). New York, NY: Springer. In press.

Jacobsen S, Iversen E, Knutti D, et al. (1986) Design of the Utah/M.I.T. dextrous hand. In: *Proceedings of the 1986 IEEE International conference on robotics and automation*, pp. 1520–1532.

Jau BM (1995) Dexterous telemanipulation with four fingered hand system. In: *Proceedings of the 1995 IEEE International conference on robotics and automation*, pp. 338–343.

Kinoshita H, Backstrom L, Flanagan JR, et al. (1997) Tangential torque effects on the control of grip forces when holding objects with a precision grip. *Journal of Neurophysiology* 78(3): 1619.

Kurse M, Lipson H and Valero-Cuevas FJ (2012) Extrapolatable analytical functions for tendon excursions and moment arms from sparse datasets. *IEEE Transactions on Biomedical Engineering* 6(59): 1572–1582.

Kutch JJ and Valero-Cuevas FJ (2012) Challenges and new approaches to proving the existence of muscle synergies of neural origin. *PLoS Computational Biology*. 8(5): e1002434.

Kutch JJ and Valero-Cuevas FJ (2011) Muscle redundancy does not imply robustness to muscle dysfunction. *Journal of Biomechanics* 44(7): 1264–1270.

Lee JJ and Tsai LW (1991) The structural synthesis of tendon-driven manipulators having a pseudotriangular structure matrix. *The International Journal of Robotics Research* 10(3): 255.

MacKenzie CL and Iberall T (1994) *The Grasping Hand* (*Advances in Psychology*, vol. 104). Amsterdam: North-Holland.

Massa B, Roccella S, Carrozza MC, et al. (2002) Design and development of an underactuated prosthetic hand. In: *Proceedings of the 2002 IEEE International conference on robotics and automation*, pp. 3374–3379.

Miller AT and Allen PK (1999) Examples of 3D grasp quality computations. In: *Proceedings of the 1999 IEEE International conference on robotics and automation*.

Murray RM, Li Z and Sastry SS (1994) *A Mathematical Introduction to Robotic Manipulation*. Boca Raton, FL: CRC.

Ou YJ and Tsai LW (1993) Kinematic synthesis of tendon-driven manipulators with isotropic transmission characteristics. *Journal of Mechanical Design* 115: 884.

Ou YJ and Tsai LW (1996) Isotropic design of tendon-driven manipulators. *Journal of Mechanical Design* 118(3): 360–366.

Pearlman JL, Roach SS and Valero-Cuevas FJ (2004) The fundamental thumb-tip force vectors produced by the muscles of the thumb. *Journal of Orthopaedic Research* 22(2): 306–312.

Pollard NS and Gilbert RC (2002) Tendon arrangement and muscle force requirements for humanlike force capabilities in a robotic finger. *Environment* 17: 14.

Porter R, Lemon R and Physiological S (1993) *Corticospinal Function and Voluntary Movement*. Oxford: Clarendon Press.

Salisbury JK and Craig JJ (1982) Articulated hands: Force control and kinematic issues. *The International Journal of Robotics Research* 1(1): 4.

Santos VJ and Valero-Cuevas FJ (2006) Reported anatomical variability naturally leads to multimodal distributions of

Denavit-Hartenberg parameters for the human thumb. *IEEE Transactions on Biomedical Engineering* 53(2): 155–163.

Santos VJ, Bustamante CD and Valero-Cuevas FJ (2009) Improving the fitness of high-dimensional biomechanical models via data-driven stochastic exploration. *IEEE Transactions on Biomedical Engineering* 56(3): 552–564.

Sheu JB, Huang JJ and Lee JJ (2009) Kinematic synthesis of tendon-driven robotic manipulators using singular value decomposition. *Robotica* 28(1): 1–10.

Shirafuji S, Ikemoto S and Hosoda K (2012) Design of an anthropomorphic tendon-driven robotic finger. In: *2012 IEEE International conference on robotics and biomimetics (ROBIO)*, pp. 372–377.

Theodorou EA (2011) *Iterative path integral stochastic optimal control: Theory and applications to motor control*. PhD Thesis, University of Southern California, USA.

Tsai LW (1995) Design of tendon-driven manipulators. *Journal of Mechanical Design* 117: 80.

Valero-Cuevas FJ (2005) An integrative approach to the biomechanical function and neuromuscular control of the fingers. *Journal of Biomechanics* 38(4): 673–684.

Valero-Cuevas FJ (2009) A mathematical approach to the mechanical capabilities of limbs and fingers. In: *Progress in Motor Control*. US: Springer, pp. 619–633.

Valero-Cuevas FJ, Hoffmann H, Kurse MU, et al. (2009) Computational models for neuromuscular function. *IEEE Reviews in Biomedical Engineering* 2: 110–135.

Valero-Cuevas FJ, Johanson ME and Towles JD (2003) Towards a realistic biomechanical model of the thumb: The choice of kinematic description may be more critical than the solution method or the variability/uncertainty of musculoskeletal parameters. *Journal of Biomechanics* 36(7): 1019–1030.

Valero-Cuevas FJ, Towles JD and Hentz VR (2000) Quantification of fingertip force reduction in the forefinger following simulated paralysis of extensor and intrinsic muscles. *Journal of Biomechanics* 33(12): 1601–1609.

Valero-Cuevas FJ, Yi JW, Brown D, et al. (2007) The tendon network of the fingers performs anatomical computation at a macroscopic scale. *IEEE Transactions on Biomedical Engineering* 54(6): 1161–1166.

Valero-Cuevas FJ, Zajac FE and Burgar CG (1998) Large index-fingertip forces are produced by subject-independent patterns of muscle excitation. *Journal of Biomechanics* 31(8): 693–704.

Vande Weghe M, Rogers M, Weissert M, et al. (2004) The act hand: Design of the skeletal structure. In: *Proceedings of the 2004 IEEE International conference on robotics and automation*, pp. 3375–3379.

Von Adolph H (1968) 1 Form und Funktion der Primatenhände. *Handgebrauch und Verständigung bei Affen und Frühmenschen*, pp. 9–30.

Wilson FR (2010) *The hand: How its use shapes the brain, language, and human culture*. New York, NY: Random House Digital, Inc.

Zajac FE (1989) Muscle and tendon: Properties, models, scaling, and application to biomechanics and motor control. *Critical Reviews in Biomedical Engineering* 17(4): 359.